Advanced Composite Materials
Publication details, including instructions for authors and subscription information:
http://www.tandfonline.com/loi/tacm20

Effects with a matrix crack on monitoring by electrical resistance method

Akira Todoroki , Miho Tanaka , Yoshinobu Shimamura & Hideo Kobayashi

Version of record first published: 02 Apr 2012.

To cite this article: Akira Todoroki , Miho Tanaka , Yoshinobu Shimamura & Hideo Kobayashi (2004): Effects with a matrix crack on monitoring by electrical resistance method, Advanced Composite Materials, 13:2, 107-120

To link to this article: http://dx.doi.org/10.1163/1568551041718071

Adv. Composite Mater., Vol. 13, No. 2, pp. 107–120 (2004)

Also available online - www.vsppub.com

Effects with a matrix crack on monitoring by electrical resistance method

AKIRA TODOROKI *, MIHO TANAKA, YOSHINOBU SHIMAMURA and HIDEO KOBAYASHI

Department of Mechanical Sciences and Engineering, Tokyo Institute of Technology, 2-12-1, Ohokayama, Meguro-ko, Tokyo 152-8552, Japan

Received 27 August 2003; accepted 1 March 2004

Abstract—Delamination engenders low reliability for primary structures because delaminations of composite laminates are usually invisible or difficult to detect by visual inspections. Automatic systems for in-service delamination identifications are desired to improve this low reliability. The present study employs an electric resistance change method for detection of delaminations. Although the method is effective in monitoring delamination cracks, it requires many experiments to solve inverse problems. An analytical method for preparation of data sets of the electric resistance changes is desired because the experimental cost is high. However, actual delamination cracks usually include matrix cracking. Therefore, this study uses FEM analyses to investigate the effect of matrix cracking on electric resistance changes between electrodes. Results show that simple calculations using a straight delamination crack model are sufficient to obtain the data set of electric resistance changes to calculate response surfaces.

Keywords: CFRP smart structure; electric resistance; response surface; FEM.

1. INTRODUCTION

Many aerospace structural components adopt CFRP structures because Carbon Fiber Reinforced Plastic (CFRP) laminates offer superior properties, such as specific strength and specific stiffness. Unfortunately, such CFRP structures have low delamination resistance. This low delamination resistance engenders delamination cracks caused by slight impacts, such as by a tool dropping. Delamination causes low reliability for primary structures of laminated composites because delamination cracks are difficult to detect in visual inspections. Identification of delamination cracks in-service is required to improve this low reliability. A health monitoring

*To whom correspondence should be addressed. E-mail: atodorok@ginza.mes.titech.ac.jp

system to detect delamination cracks is one desirable approach for practical laminated composite structures.

Recently, many researchers have demonstrated the advantage of an electrical resistance method for monitoring damage to structures [1–9]. Both experimentally and analytically, authors have demonstrated the applicability of the electric resistance change method to identify location and size of a delamination crack in a CFRP laminate [10–15]. For those results, authors have adopted response surfaces as a tool for solution of inverse problems. That method is applied to CFRP laminated plates with multiple electrodes mounted on the single surface. Electrical resistance changes of various locations and sizes of delamination cracks are measured between adjacent electrodes; thereupon, inverse analyses with response surfaces identify the delamination crack from the measured electric resistance changes. This method uses the response surface to solve inverse problems. For that reason, it requires many experiments to determine all coefficients of response surfaces with the least-squares error method. The delamination location or size is regressed using a quadratic polynomial with measured electric resistance changes.

Conducting numerous experiments is very expensive in practical applications. Rather than conducting these expensive experiments, FEM analyses to obtain electric resistance changes are preferable in terms of reduced cost. It is crucial to know the effect of matrix cracking on electric resistance changes because actual delamination cracks usually involve matrix cracking and have various shapes that result from matrix cracking. To simplify FEM analysis, it is desirable to use a straight delamination crack without a matrix crack. Calculating many delamination shapes is onerous even though actual delamination cracks have many different zigzag shapes produced by the matrix cracks.

Therefore, FEM analyses are performed in this study to investigate the effect of matrix cracking on electric resistance changes caused by a delamination of laminated CFRP beams. Cross-ply CFRP laminates are used for FEM analyses. For cross-ply laminates, a delamination crack usually involves a matrix crack; moreover, the delamination crack shape is not straight. The present study calculates electrical resistance changes caused by a zigzag-shaped delamination with a matrix crack and compares them with results for a straight delamination crack. Response surfaces to estimate delamination location and size are produced from FEM results obtained with a straight delamination crack. Estimations of delamination location and size of the zigzag delamination cracks with matrix cracks are performed with response surfaces produced from results for straight delamination cracks. Effects of matrix cracking on estimation performance are discussed based on these results.

2. FEM ANALYSES OF MATRIX CRACK EFFECTS

2.1. Analytical method

In this study, FEM analyses were performed with the commercially available FEM code ANSYS. Beam type specimens were adopted for FEM analyses of

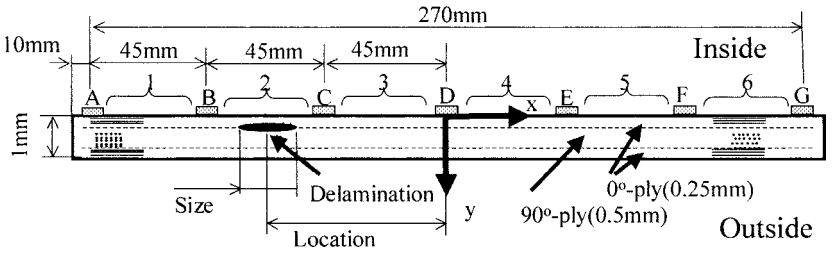

Figure 1. Specimen [0/90]s.

Table 1.
Conductivity ratio

V_f	σ_{90}/σ_0	σ_t/σ_0	σ_0 ($m^{-1}\,\Omega^{-1}$)
0.621	3.71×10^{-2}	3.77×10^{-3}	5.5×10^3

delamination monitoring, as shown in Fig. 1. The specimen stacking sequence is [0/90]s. The specimen length is 290 mm and the beam height (CFRP laminate thickness) is 1 mm. Seven 5-mm-wide electrodes are mounted on the specimen surface; spacing of electrodes is 45 mm. Four-node rectangular elements are used for FEM analyses: length of an element is 0.25 mm and its approximate height is 0.0625 mm.

A direct current of 30 mA is charged at one electrode and the electrical voltage of the other electrode is set to 0 V to measure electrical resistance change between adjacent electrodes. Switching the charging segment, each electrical resistance change of segment $\Delta R_i/R_{i0}$ ($i = 1, 2, \ldots, 6$) is obtained from the calculated voltage change. For each type of specimen in the present study, multiple electrodes are mounted on a single surface of the specimen. The reason for placement of all electrodes on the same surface is to simulate identification of an invisible internal delamination crack by mounting electrodes on the inner surface of a shell-type structure such as an aircraft. Therefore, the specimen surface where all electrodes are mounted is called inside, and the other surface is called outside in this paper.

Table 1 shows orthotropic electrical conductivity used in these FEM analyses. Results are derived from experimental results of reference [15]. In this table, V_f is fiber volume fraction, σ_0 is electrical conductivity of the fiber direction, σ_{90} is electrical conductivity of the transverse direction, and σ_t represents electrical conductivity of the thickness direction.

2.1.1. Standardization of electrical resistance change. Our previous paper [16] reports that electrical resistance changes obtained from FEM analyses include information about both delamination location and size: delamination crack distance from the electrode is inversely related to electrical resistance; delamination size is directly related to electrical resistance. These relations engender a large scatter band of estimations of delamination location. A standardization method has been proposed in our previous paper to prevent the large scatter band. A set of electrical

resistance changes of the six segments is regarded as a vector comprising six elements wherein each vector element is standardized with the vector length. The standardized electrical resistance change is defined as the following:

$$\frac{\Delta r_i}{r_{i0}} = \frac{\Delta R_i / R_{i0}}{\sqrt{\sum_{k=1}^{6} (\Delta R_k / R_{k0})}} \quad (i = 1, \ldots, 6). \tag{1}$$

Details of that equation are explained in our previous paper [16].

2.1.2. Zigzag delamination resulting from matrix cracking. Most actual delamination cracks include matrix cracking and have a zigzag shape instead of a straight crack. Many delamination patterns are created by matrix cracking. It is, however, preferable to calculate only straight delamination models without matrix cracking for FEM analyses. Therefore, this study uses a straight delamination crack like that shown in Fig. 1 to create response surfaces to estimate delamination location and size.

A delamination crack is usually made near the surface; it is located opposite from the impacted surface. A delamination crack should be made at the interface near the inside surface to simulate this delamination location. In this study, the outside surface is the bottom surface and the inside surface is the top surface, as shown in Fig. 1. That figure shows a delamination crack that is made at the interface between the top 0° ply and the middle 90° ply. All nodes are doubly defined to represent delamination crack surfaces on delamination crack surface lines. When a delamination crack is created, doubly defined nodes on delamination crack surfaces are released with each other to represent electric current insulation. For a delamination crack induced in the FEM model, the present study subsumes that the crack mouth is fully opened after delamination, although an actual delamination crack has crack surface contact. Five kinds of delamination sizes are calculated here: 5, 10, 20, 30, and 40 mm. Many patterns of delamination location are calculated for each delamination size: spacing between adjacent patterns of delamination location is 5 mm. The total number of FEM calculations is 263 for the straight delamination crack.

Zigzag delamination cracks with a matrix crack are modeled as shown in Fig. 2 to elucidate effects of matrix cracking. The present study uses a zigzag delamination which has a delamination between the top 0° ply and the middle 90° ply in the left side of the matrix crack in the middle 90° ply and has a delamination between the bottom 0° ply and the middle 90° ply in the right side of the matrix crack. This delamination, as shown in Fig. 2a, is called a Z-type crack because its pattern resembles a letter 'Z'. An inverted zigzag pattern, as shown in Fig. 2b, is called an inverse-Z-type here.

Many ratios of delamination length exist between the top delamination length and the bottom one for actual Z-type and the inverse-Z-type delaminations. Three types of ratios are adopted in the present study: 90/10, 50/50, and 10/90. In the

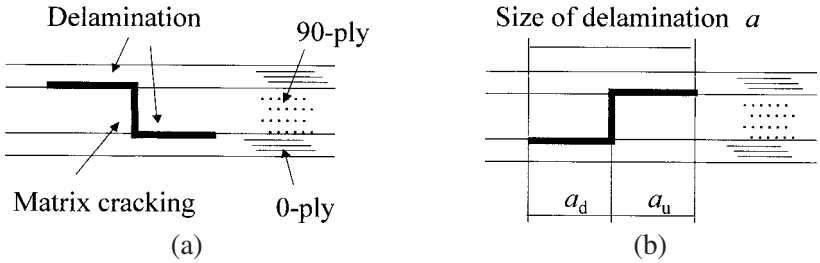

Figure 2. Configuration of the delamination with matrix cracking. (a) Z type. (b) Inverse-Z type.

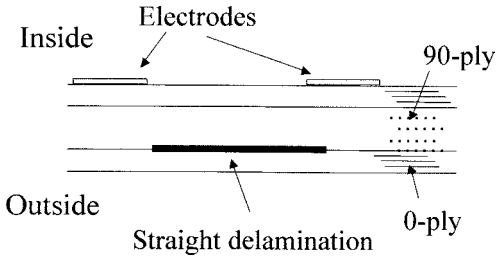

Figure 3. Configuration of the downside delamination crack.

present study, the size of these delaminations indicates the projected length as shown in Fig. 2. The delamination location is the center location of the projected delamination. Moreover, as an extreme case, a pattern that has a delamination between the bottom 0° ply and the middle 90° ply, as shown in Fig. 3, is prepared for analyses; nevertheless, this pattern is a rare case among actual delaminations because matrix cracking is a trigger for making most of the actual delaminations.

2.2. FEM results

2.2.1. Electrical resistance difference caused by the delamination shape pattern. Figure 4 shows FEM analysis results in this case: the delamination locates at $x = 0$ mm and the length is 5 mm. The abscissa is the segment number between the adjacent electrodes; the ordinate is the standardized electrical resistance change. Solid symbols represent results for straight delamination. Other Z-type delaminations of three ratios (open circles: 90/10, open triangles: 50/50 and open diamonds: 10/90) are shown in Fig. 4. Figure 5 shows results of FEM analyses of the case: the delamination locates at $x = -40$ mm and the length is 5 mm. In Fig. 5, four results are shown similar to Fig. 4.

Figures 4 and 5 show that electrical resistance changes of the Z-type delamination cracks differ from the straight delamination crack in both delamination locations. The largest difference is observed in the Z-type delamination of the ratio of 50/50. That ratio is fixed to 50/50 in the latter half of the present paper because the greatest difference is observed for delamination with a 50/50 ratio.

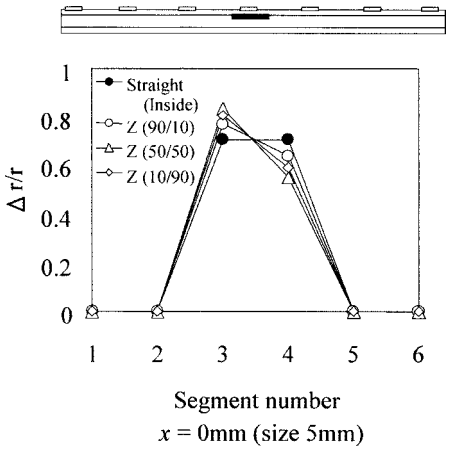

Figure 4. Electric resistance changes for straight and Z-type delamination cracks (location 0 mm, size 5 mm).

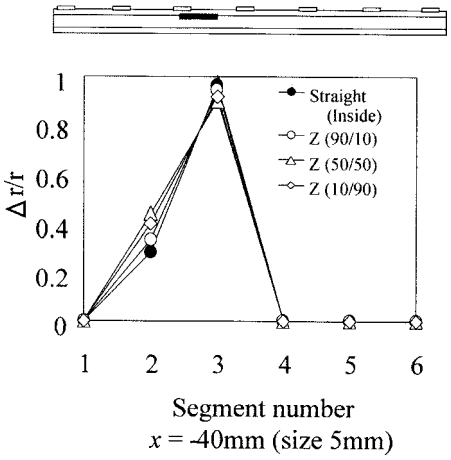

Figure 5. Electric resistance changes for straight and Z-type delamination cracks (location −40 mm, size 5 mm).

Figures 6 and 7 show comparisons between upside (inside) delamination and downside (outside) delamination for straight delamination cracks. In Fig. 6, the 5-mm delamination is located at $x = 0$ mm. In Fig. 7, the 5-mm delamination is located at the point of $x = -40$ mm. Locations of those delaminations are the same as those of Figs 4 and 5, respectively. Figures 6 and 7 show no difference between results. This similarity means that the difference of the electrical resistance changes observed in Figs 4 and 5 is caused by existence of a matrix crack. Figures 8 and 9 show the results of the cases in which the largest differences where observed. The next section presents discussion of the effect of matrix cracking on estimations.

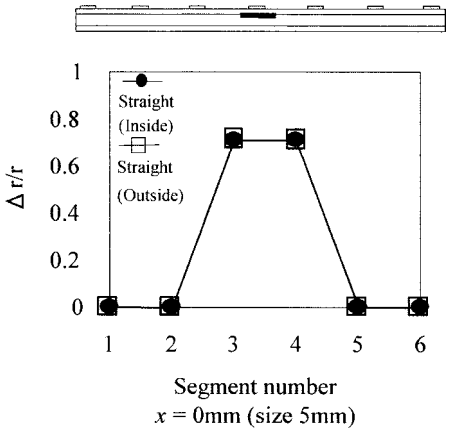

Figure 6. Electric resistance changes for inside and outside delamination (location 0 mm, size 5 mm).

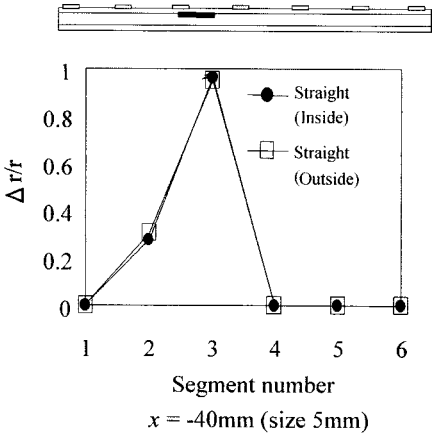

Figure 7. Electric resistance changes for inside and outside delamination (location −40 mm, size 5 mm).

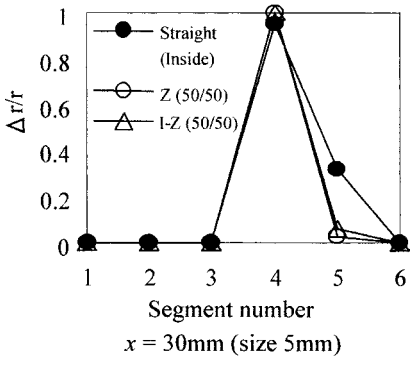

Figure 8. Example of largest difference of electric resistance changes (location 30 mm, size 5 mm).

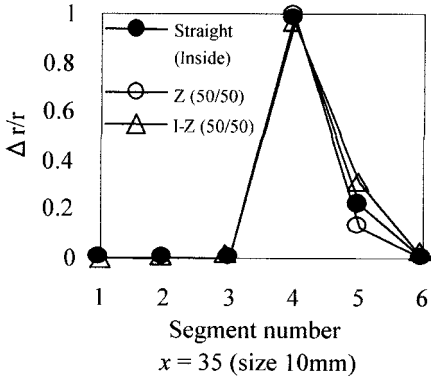

Figure 9. Example of largest difference of electric resistance changes (location 35 mm, size 10 mm).

3. EFFECT OF MATRIX CRACKING ON ESTIMATIONS

3.1. Response surface methodology

The response surface is a widely adopted tool for quality engineering fields. Response surface methodology comprises a regression curve fitting to obtain approximate responses, design of experiments to obtain minimum variances of responses, and optimizations using approximated responses.

The present study adopts response surface methodology as a solution for inverse problems. For this study, predictions of delamination locations and sizes from measured electric resistance changes are one inverse problem. Response surface methodology offers two advantages: inverse problems can be solved approximately without consideration of modeling; also, approximated response surfaces can be evaluated using statistical tools.

Functions for approximations for most response surfaces are polynomials because of their simplicity. For cases of quadratic polynomials, the response surface is described as

$$y = \beta_0 + \sum_{j=1}^{k} \beta_j x_j + \sum_{j=1}^{k} \beta_{jj} x_j^2 + \sum_{i=1}^{k-1} \sum_{j=i+1}^{k} \beta_{ij} x_i x_j, \tag{2}$$

where k is the number of variables, x represents variables, y is a response, and β represents unknown coefficients.

Through substitution of square terms and interaction terms with new variables such as $x_i x_j = x_m$, equation (2) assumes the form of a linear regression model. The coefficients can be calculated with the least-squares error method.

In the case where the total number of experiments is n, the response surface can be expressed as follows using a matrix expression:

$$\mathbf{Y} = \mathbf{X}\boldsymbol{\beta} + \mathbf{e}, \tag{3}$$

where

$$\mathbf{Y} = \begin{Bmatrix} y_1 \\ y_2 \\ \vdots \\ y_n \end{Bmatrix}, \quad \mathbf{X} = \begin{bmatrix} 1 & x_{11} & x_{12} & \cdots & x_{1k} \\ 1 & x_{21} & x_{22} & \cdots & x_{2k} \\ \vdots & \vdots & \vdots & \ddots & \vdots \\ 1 & x_{n1} & x_{n2} & \cdots & x_{nk} \end{bmatrix},$$

and

$$\boldsymbol{\beta} = \begin{Bmatrix} \beta_0 \\ \beta_1 \\ \vdots \\ \beta_k \end{Bmatrix}, \quad \mathbf{e} = \begin{Bmatrix} \varepsilon_1 \\ \varepsilon_2 \\ \vdots \\ \varepsilon_n \end{Bmatrix},$$

and $\mathbf{e}$ is an error vector.

The unbiased estimator $\mathbf{b}$ of the coefficient vector $\boldsymbol{\beta}$ is obtained using the well known least-squares error method.

$$\mathbf{b} = (\mathbf{X}^T\mathbf{X})^{-1}\mathbf{X}^T\mathbf{Y}. \tag{4}$$

The adjusted coefficient of multiple determination R^2_{adj} is used to judge goodness of approximation of the response surface.

$$\begin{aligned} R^2_{\text{adj}} &= 1 - \frac{SS_E/(n-k-1)}{S_{yy}/(n-1)}, \\ SS_E &= \mathbf{Y}^T\mathbf{Y} - \mathbf{b}^T\mathbf{X}^T\mathbf{Y}, \\ S_{yy} &= \mathbf{Y}^T\mathbf{Y} - \frac{\left(\sum_{i=1}^{n} y_i\right)^2}{n}. \end{aligned} \tag{5}$$

In those equations, SS_E is the square sum of errors and S_{yy} is the total sum of squares. Each coefficient of the response surface can be tested using the t-statistic. When the absolute value of t-statistics is smaller than the threshold value of the t-distribution ($t_{0.025,n-k-1}$), the coefficient is eliminated from the response surface as an unimportant coefficient for obtaining higher R^2_{adj}. The fitness of the regressed surfaces of the different degree of freedom can be compared using the R^2_{adj}.

Two response surfaces are made in this study: one estimates the delamination location; the other estimates the delamination size. All coefficients of the response surfaces are calculated from the 263 FEM results. Six standardized electrical resistances are used for estimations of delamination locations. Six standardized electrical resistance changes and the length used for standardization are used for estimations of delamination size.

3.2. Estimation procedure for Z-type and inverse Z-type delaminations

In Section 2, electric resistance changes of the straight delamination crack are shown to differ from those of the Z-type delamination crack. This section presents a discussion of the effect of different electrical resistance changes on estimations. The estimation procedure is described as follows.

(1) Two response surfaces to estimate delamination location and size are made from the 263 FEM results calculated using straight delamination cracks of five sizes: 5, 10, 20, 30, and 40 mm.
(2) FEM analyses of Z-type and inverse-Z-type of the ratio of 5/5 are performed to obtain electrical resistance changes.
(3) Obtained results of Z-type and inverse Z-type delaminations are substituted into the two response surfaces obtained; then delamination location and size are estimated for the Z-type and the inverse Z-type delamination cracks.
(4) Obtained estimated results are compared with those for the true delamination crack used for FEM analyses.

3.3. Estimations of the straight delamination crack

Figure 10 shows results of estimations of straight delamination location used for making the response surface. Figure 11 shows results of estimations of straight delamination size used for making the response surface. In these figures, the

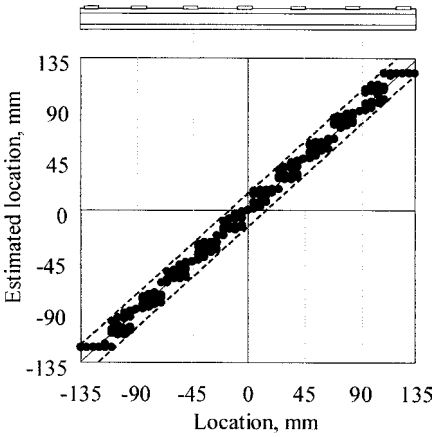

Figure 10. Results of estimation of straight delamination cracks (location).

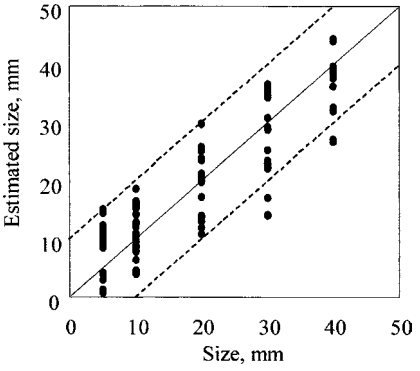

Figure 11. Results of estimation of straight delamination cracks (size).

abscissa is the true delamination location or size and the ordinate is the estimated delamination location and size. Plots located on the diagonal line indicate exact estimations. The R^2_{adj} of delamination location (Fig. 10) is 0.994; the R^2_{adj} of delamination size (Fig. 11) is 0.807.

An error band of 15 mm from the exact estimation is shown as dashed lines in Fig. 10. As shown in Fig. 10, almost all estimations of delamination locations can be plotted within the error band of 15 mm. The error band of most estimation is less than 10 mm. In Fig. 11, an error band of 10 mm from the exact estimation is shown using dashed lines. As shown in Fig. 11, almost all estimations of delamination size can be plotted within the error band of 10 mm. These results show the effectiveness of the standardization method, as shown in our previous paper [16].

3.4. Estimations of Z-type and inverse-Z-type delaminations

First of all, FEM results of the electrical resistance changes of Z-type and inverse Z-type shown in Figs 4 and 5, respectively, are substituted into response surfaces to estimate delamination location and size: response surfaces are made from FEM results for straight delamination cracks. Figure 12 shows the estimated results for delamination location. Figure 13 shows the estimated results of delamination size. In these figures, the abscissas show the true location or size and the ordinates are the estimated location or size. The figures show: solid circle symbols, representing results of the straight delamination cracks; open circle symbols, representing results of the Z-type delamination cracks; and open triangle symbols representing results for inverse Z-type delamination cracks. Dotted lines in Fig. 12 indicate the error band of 15 mm that is obtained from estimation results of the straight delamination cracks in Fig. 10. Similarly, dotted lines in Fig. 13 designate the error band of 10 mm that is obtained in Fig. 11. These estimation results show that estimated results of the Z-type and the inverse Z-type differ from the case of the straight delamination crack. Notwithstanding, the estimations exist within error bands in both estimations.

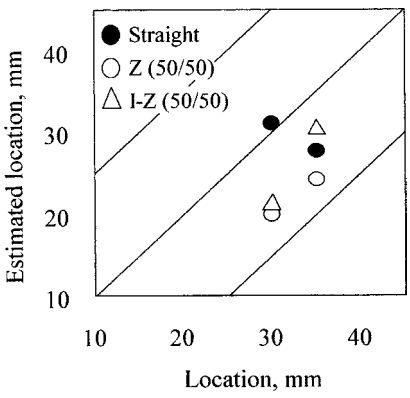

Figure 12. Results of estimations of the largest difference of electric resistance changes observed in Figs 8 and 9 (location).

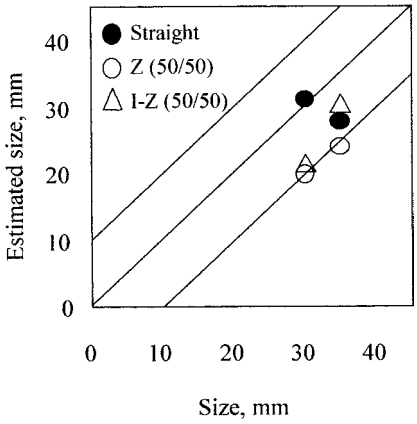

Figure 13. Results of estimations of the largest difference of electric resistance changes observed in Figs 8 and 9 (size).

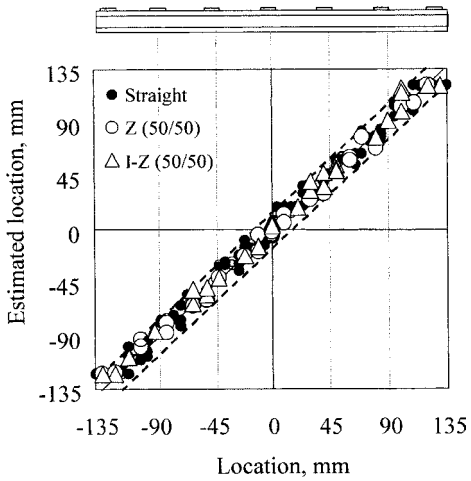

Figure 14. Results of estimations of zigzag delamination cracks using the response surface obtained from the straight delamination cracks (location).

These small errors that result from matrix cracking indicate that the response surfaces can be produced from FEM results of the straight delamination cracks.

Many FEM analyses of Z-type and inverse Z-type were performed to confirm this: five delamination sizes (5, 10, 20, 30, and 40 mm) and six cases of locations for each length were randomly selected (30 cases for each). These FEM results are substituted into the response surfaces to estimate the delamination location and size similarly. Figure 14 shows results of estimations of the delamination location. Figure 15 shows results of estimations of the delamination size. Estimations of straight delamination cracks are shown with small solid-circle symbols. Open circle symbols represent estimations of Z-type delamination cracks; triangle symbols represent inverse Z-type delamination cracks. In these figures, abscissas are the true

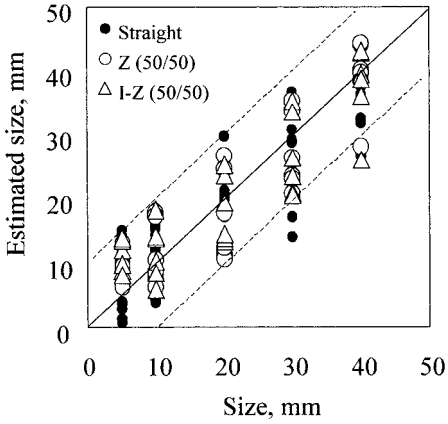

Figure 15. Results of estimations of zigzag delamination cracks using the response surface obtained from the straight delamination cracks (size).

delamination location or size and ordinates are the estimated delamination location or size, respectively. As with results of Figs 12 and 13, all estimations of the Z-type and the inverse Z-type differ from estimations of straight delamination cracks. All estimations exist within the error bands. These results reveal that the matrix crack effect is negligible, but the matrix cracking affects electric resistance changes.

These results show that matrix cracking of actual delamination cracks affects electrical resistance changes slightly. Response surfaces made from FEM results of straight delamination cracks are sufficiently robust. It is unnecessary to consider various delamination shapes, such as Z-type and inverse Z-type, to produce response surfaces for cross-ply laminates.

4. CONCLUSIONS

This study conducted FEM analyses to investigate the effect of matrix cracking on electric resistance changes caused by a delamination of laminated CFRP beams. Electrical resistance changes caused by a zigzag delamination with a matrix crack were calculated and compared with results for a straight delamination crack. Actual delamination with a matrix crack is called a Z-type delamination crack here because the zigzag resembles a letter Z. Discussion of the effect of the matrix crack on estimations is performed on the basis of those results. Results obtained are the following.

(1) For actual delamination cracks with matrix cracking, electric resistance changes differ from results obtained from straight delamination cracks.

(2) Electrical resistance changes of the Z-type delamination crack differ from those of the inverse Z-type delamination crack.

(3) Although slight differences exist between electrical resistance changes, response surfaces may be made from FEM results of straight delamination cracks.

In addition, response surfaces provide reasonable estimations within error bands of the straight delamination cracks, even for actual delamination cracks with matrix cracking such as the Z-type delamination cracks.

REFERENCES

1. K. Schulte and Ch. Baron, Load and failure analyses of CFRP laminates by means of electrical resistivity measurements, *Compos. Sci. Technol.* **36** (1), 63–76 (1989).
2. C. N. Owston, Eddy current methods for the examination of carbon fiber reinforced epoxy resins, *Materials Evaluation* **34** (11), 237–244 (1976).
3. T. Sakagami, S. Kubo and K. Ohji, Crack identification by the electric potential CT inverse analyses incorporating optimization techniques, *Engineering Analysis with Boundary Elements* **7** (2), 59–65 (1990).
4. S. Kubo, M. Kuchinishi, T. Sakagami and S. Ioka, Identification of delamination in layered composite materials by the electric potential CT method, *Intern. J. Appl. Electromagnetics Mech.* **15** (1/4), 261–268 (2002).
5. N. Tada, Y. Hayashi, T. Kitamura and R. Ohtani, Analysis on the applicability of direct current electrical potential method to the detection of damage by multiple small internal cracks, *Intern. J. Fracture* **85** (1), 1–9 (1997).
6. P. W. Chen and D. D. L. Chung, Carbon-fiber-reinforced concrete as intrinsically smart concrete for damage assessment during dynamic loading, *J. Am. Ceram. Soc*. **78** (3), 816–818 (1995).
7. X. Wang and D. D. L. Chung, Sensing delamination in a carbon fiber polymer-matrix composite during fatigue by electrical resistance measurement, *Polym. Compos.* **18** (6), 692–700 (1997).
8. J. C. Abry, Y. K. Choi, A. Chateuminois, B. Dalloz and G. Giraud, In-situ monitoring of damage in CFRP laminates by means of AC and DC measurements, *Compos. Sci. Technol.* **61**, 855–864 (2001).
9. R. Schueler, S. P. Joshi and K. Schulte, Damage detection in CFRP by electrical conductance mapping, *Compos. Sci. Technol.* **61**, 921–930 (2001).
10. A. Todoroki, K. Matsuura and H. Kobayashi, Application of electric potential method to smart composite structures for detecting delamination, *JSME Intern. J., Series A* **38** (4), 524–530 (1995).
11. A. Todoroki, H. Kobayashi and K. Matsuura, Application of electrical potential method as delamination sensor for smart structures of graphite/epoxy, in: *US–Japan Workshop on Smart Materials and Structures*, K. Inoue, S. I. Y. Shen and M. Taya (Eds), pp. 47–54. University of Washington TMS (1997).
12. A. Todoroki and H. Suzuki, Evaluation of orthotropic electrical resistance for delamination smart detection of graphite/epoxy composites by electrical potential method, in: *Proc. 1st Asian–Australian Conference on Composite Materials* (ACCM-1), pp. 630(1)–630(4) (1998).
13. A. Todoroki and H. Suzuki, Health monitoring of internal delamination cracks for graphite/epoxy composites by electric potential method, *Appl. Mech. Engng* **5** (1), 283–294 (2000).
14. A. Todoroki, Effect of number of electrodes and diagnostic tool for delamination monitoring of graphite/epoxy laminates using electric resistance change, *Compos. Sci. Technol.* **61** (13), 1871–1880 (2001).
15. A. Todoroki, M. Tanaka and Y. Shimamura, Measurement of orthotropic electric conductance of CFRP laminates and analysis of the effect on delamination monitoring with electric resistance change method, *Compos. Sci. Technol.* **62** (56), 19–28 (2002).
16. A. Todoroki, M. Tanaka and Y. Shimamura, High performance estimations of delamination of graphite/epoxy laminates with electric resistance change method, *Compos. Sci. Technol.* **63** (13), 1911–1920 (2003).